DOI: 10.1007/s11099-012-0057-z PHOTOSYNTHETICA 50 (4): 529-540, 2012

Light-dependent and light-independent protochlorophyllide oxidoreductases share similar sequence motifs – *in silico* studies

M. GABRUK[*], J. GRZYB[**], J. KRUK[*,+], and B. MYSLIWA-KURDZIEL[*]

Department of Plant Physiology and Biochemistry, Faculty of Biochemistry, Biophysics and Biotechnology, Jagiellonian University, ul. Gronostajowa 7, 30-387 Kraków, Poland[*]
Laboratory of Biological Physics, Institute of Physics PAS, al. Lotników 32/46, 02-668 Warsaw, Poland[**]

Abstract

In the present studies, we have found a fragment of amino acid sequence, called TFT motif, both in light-dependent protochlorophyllide oxidoreductase (LPOR) and in the L subunit of dark-operative (light-independent) protochlorophyllide oxidoreductases (DPOR). Amino acid residues of this motif shared similar physicochemical properties in both types of the enzymes. In the present paper, physicochemical properties of amino acid residues of this common motif, its spatial arrangement and a possible physiological role are being discussed. This is the first report when similarity between LPOR and DPOR, phylogenetically unrelated, but functionally redundant enzymes, is described.

Additional key words: chlorophyll biosynthesis, homology modeling, protochlorophyllide, protochlorophyllide oxidoreductase, sequence analysis.

Introduction

Reduction of protochlorophyllide (Pchlide) to chlorophyllide (Chlide) is the key step in chlorophyll and bacteriochlorophyll biosynthesis (Fig. 1) (Masuda 2008). As a result of this reaction, one double bond of the Pchlide molecule is reduced and Chlide is formed. Two types of enzymes catalyzing Pchlide reduction exist. In photosynthetic anoxygenic bacteria, only light-independent, dark-operative protochlorophyllide oxidoreductase (DPOR) is found. On the other hand, in angiosperms only a photoenzyme NADPH:Pchlide oxidoreductase (LPOR) occurs and Pchlide to Chlide conversion is strictly light-dependent (Schoefs and Franck 2003). In other photosynthetic organisms both enzymes are present.

It is generally assumed that LPOR and DPOR belong to different enzyme families and have evolved independently. LPOR is a single-chain, nuclear-encoded protein belonging to the family of short chain dehydrogenases/reductases (SDR) (Yang and Cheng 2004, Reinbothe *et al.* 2010). It shows a regulatory function in angiosperm development, namely in the induction of deetiolation (Schoefs and Franck 2003, Schoefs 2005, Belyaeva and Litvin 2007). LPOR is also in the focus of attention as a model of oxidoreductases (Heyes and Hunter 2005, Sytina *et al.* 2009).

DPOR consists of three protein subunits, which are products of *bchL/chlL*, *bchB/chlB*, and *bchN/chlN* genes, in bacteria/plants. The subunits of DPOR show significant sequence homology with three subunits of nitrogenase (Masuda 2008, Reinbothe *et al.* 2010) catalyzing the formation of ammonia from dinitrogen (Igarashi and Seefeldt 2003). $[BchB–BchN]_2$ heterotetramer (NB-protein) and $[BchL]_2$ dimer (L-protein) form the functional DPOR macrodomain and function as the catalytic and reductase components, respectively (Schoefs and Franck 2003, Masuda 2008, Reinbothe *et al.* 2010).

Received 20 January 2012; *accepted* 7 July 2012.
[+]Corresponding author; fax: 48 12 664 6902; e-mail: jerzy.kruk@uj.edu.pl
Abbreviations: BchB, BchL and BchN – B, L and N subunits of bacterial DPOR, respectively; ChlL - L subunit of plant DPOR, Chlide – chlorophyllide; DPOR – dark-operative (light-independent) protochlorophyllide oxidoreductase; LPOR – light-dependent protochlorophyllide oxidoreductase; NCBI – National Center for Biotechnology Information; NifH – a protomer of Fe protein of nitrogenase; Pchlide – protochlorophyllide; PDB – Protein Data Bank; PORA – one of the isoforms of LPOR; SDR – short chain dehydrogenases/reductases
Acknowledgements: This work was partially supported by grant 2011/01/B/NZ1/00119 from National Center of Science of Poland (NCN). J.G. acknowledges support by the Foundation for Polish Science, Homing Plus Programme co-financed by the European Union within the European Regional Development Fund. The Faculty of Biochemistry, Biophysics and Biotechnology of the Jagiellonian University is a beneficiary of the structural funds from the European Union (grant No: POIG.02.01.00-12-064/08 – "Molecular biotechnology for health").

Although LPOR and DPOR catalyze the same reaction, these enzymes are completely different as far as their genes, protein structure and catalytic mechanisms are concerned. Bearing in mind a possibility of functional convergence, we have compared currently known sequences of LPORs and DPORs *in silico* to investigate if there exists any sequence similarity between the enzymes, which could be useful in further analysis of their function.

Materials and methods

Sequence analysis: Several protein sequences of the L, N, and B subunits of DPOR from NCBI (National Center of Biotechnology Information) database (Pruitt *et al.* 2006) were compared to the *Arabidopsis thaliana* PORA sequence (NCBI accession number: NP_200230). Blast algorithm with default parameters set (matrix - Blosum62, penalty for opening the gap – 11, penalty for extending the gap – 1, threshold – 10, word size - 3) was used. Similar fragments between *A. thaliana* PORA sequence and L subunits of DPOR, both BchL and ChlL, have been found. No similarities were found in the case of N and B subunits of DPOR.

Then, a database was constructed by selecting all available sequences of LPOR from green plants and L subunits of DPOR (both BchL and ChlL) from NCBI protein database (status for July 15th, 2011). The database was searched for sequences termed "protochlorophyllide NADPH oxidoreductase" and "L subunit light-independent reductase", for LPOR and DPOR respectively. The hits were manually checked to remove any mismatched or partial sequences. The following criteria were used: sequences longer than 190 amino acids (*1*) and predicted involvement in Pchlide reduction (*2*). The adjusted database finally comprised 42 sequences of LPOR and 117 sequences of BchL/ChlL, fulfilling these criteria (Table 1). The NCBI protein database was searched also to find NADPH-binding SDR proteins and Fe protein of nitrogenases (NifH) that were compared to LPOR and BchL/ChlL, respectively. Then the hits were manually checked again for mismatched or partial sequences. Finally, 270 and 141 sequences of SDR and NifH, respectively, were analyzed.

The sequence alignment was performed using ClustalW (Thompson *et al.* 1994) separately for BchL/ChlL, LPOR, SDR and NifH sequences from the constructed protein sequence database. Default parameter settings were applied, *i.e.* matrix – Gonnet 250, penalty for opening the gap – 10, endgaps – excluded, penalty for extending the gap – 0.2, gap separation penalty – 4.

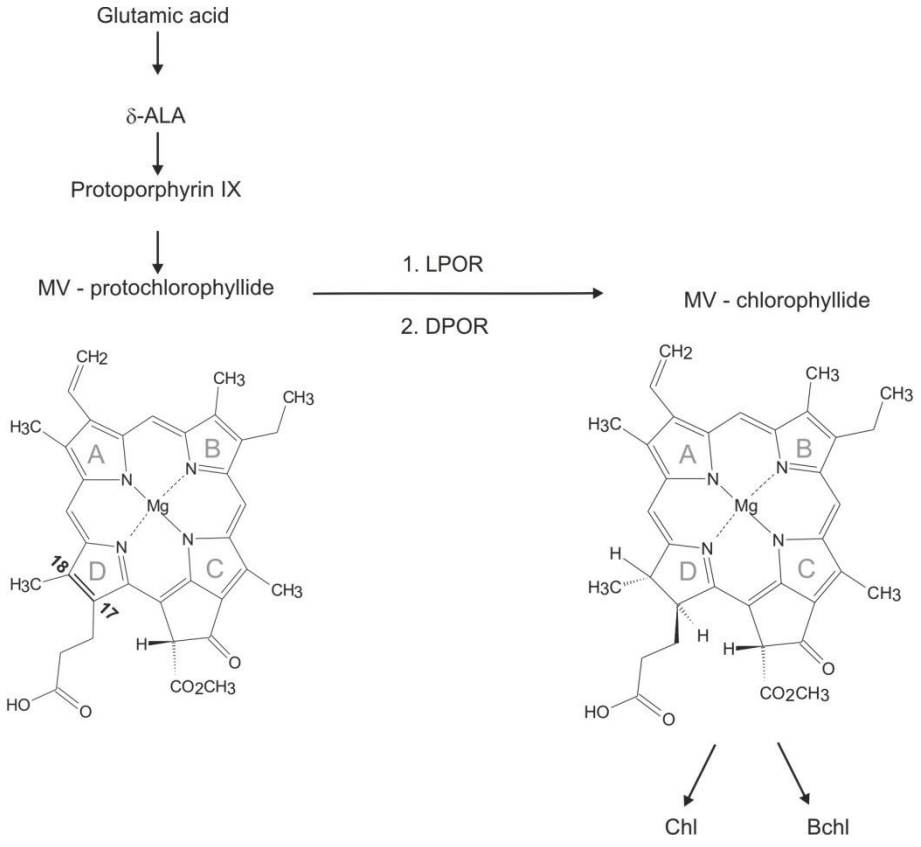

Fig. 1. Outline of the biosynthetic pathway of chlorophyll (Chl) and bacteriochlorophyll (Bchl). Reduction of the C17=C18 double bond in the pyrrole ring D of Pchlide is catalyzed by light-dependent (LPOR) or dark-operative (DPOR) Pchlide oxidoreductases. ALA – aminolevulinic acid, MV – monovinyl.

Table 1. TFT motif sequences used for the data base construction. GI numers and sourse organisms are included. The numbers in bold refer to the position of the first and the last amino acid of TFT motifs.

GI number L subunit of DPOR	Amino acid sequence			Organism
gi|3820555	**43**	TFTIAGK----------MIPTVVE	**59**	*Heliobacillus mobilis*
gi|13878359	**43**	TFTIAGK----------MIPTVVE	**59**	*Heliobacillus mobilis*
gi|226698866	**43**	TFTIAGR----------MIPTVVE	**59**	*Heliobacterium modesticaldum Ice1*
gi|167629377	**43**	TFTIAGR----------MIPTVVE	**59**	*Heliobacterium modesticaldum Ice1*
gi|167592117	**43**	TFTIAGR----------MIPTVVE	**59**	*Heliobacterium modesticaldum Ice1*
gi|41688494	**43**	TFTLTGS----------LIPTIID	**59**	*Anthoceros formosae*
gi|120542	**43**	TFTLTGF----------LIPTIID	**59**	*Marchantia polymorpha*
gi|68052070	**43**	TFTLTGF----------LIPTIID	**59**	*Huperzia lucidula*
gi|182894147	**43**	TFTLTGF----------LIPTIID	**59**	*Angiopteris evecta*
gi|68052162	**43**	TFTLTGF----------LIPTIID	**59**	*Physcomitrella patens* subsp. *patens*
gi|3913244	**43**	TFTLTGF----------LIPTIID	**59**	*Picea abies*
gi|1168937	**43**	TFTLTGF----------LIPTIID	**59**	*Pinus thunbergii*
gi|120543	**43**	TFTLTGF----------LIPTIID	**59**	*Pinus contorta*
gi|68052192	**43**	TFTLTGF----------LIPTIID	**59**	*Pinus koraiensis*
gi|68052102	**43**	TFTLTGF----------LIPTIID	**59**	*Larix decidua*
gi|172048633	**43**	TFTLTGF----------LIPTIID	**59**	*Cycas taitungensis*
gi|122211814	**43**	TFTLTGF----------LIPTIID	**59**	*Staurastrum punctulatum*
gi|122211735	**43**	TFTLTGF----------LIPTIID	**59**	*Zygnema circumcarinatum*
gi|25008287	**43**	TFTLTGF----------LIPTIID	**59**	*Chaetosphaeridium globosum*
gi|68565046	**43**	TFTLTGF----------LIPTIID	**59**	*Adiantum capillus-veneris*
gi|122224959	**43**	TFTLTGF----------LIPTIID	**59**	*Chara vulgaris*
gi|13878444	**43**	TFTLTGF----------LIPTIID	**59**	*Mesostigma viride*
gi|172045680	**43**	TFTLTGF----------LIPTIID	**59**	*Chlorokybus atmophyticus*
gi|190358902	**45**	TFTLTGF----------LIPTIID	**61**	*Synechococcus* sp. *PCC 7002*
gi|226706353	**45**	TFTLTGF----------LIPTIID	**61**	*Microcystis aeruginosa NIES-843*
gi|226706352	**45**	TFTLTGF----------LIPTIID	**61**	*Cyanothece sp. PCC 8801*
gi|120545	**45**	TFTLTGF----------LIPTIID	**61**	*Synechocystis sp. PCC 6803* substr. *Kazusa*
gi|189082380	**43**	TFTLTGF----------LIPTIID	**59**	*Acaryochloris marina MBIC11017*
gi|120544	**43**	TFTLTGF----------LIPTIID	**59**	*Leptolyngbya boryana*
gi|172046710	**43**	TFTLTGF----------LIPTIID	**59**	*Anabaena variabilis ATCC 29413*
gi|21263466	**43**	TFTLTGF----------LIPTIID	**59**	*Nostoc sp. PCC 7120*
gi|226706354	**43**	TFTLTGF----------LIPTIID	**59**	*Nostoc punctiforme PCC 73102*
gi|123056859	**43**	TFTLTGF----------LIPTIID	**59**	*Trichodesmium erythraeum IMS101*
gi|122194755	**43**	TFTLTGF----------LIPTIID	**59**	*Pyropia yezoensis*
gi|1705819	**43**	TFTLTGF----------LIPTIID	**59**	*Porphyra purpurea*
gi|254813926	**43**	TFTLTGF----------LIPTIID	**59**	*Cyanothece* sp. *PCC 7425*
gi|172045819	**43**	TFTLTGF----------LIPTIID	**59**	*Thermosynechococcus elongatus BP-1*
gi|81676983	**43**	TFTLTGF----------LIPTIID	**59**	*Synechococcus elongatus PCC 6301*
gi|1705820	**43**	TFTLTGF----------LIPTIID	**59**	*Synechococcus elongatus PCC 7942*
gi|123505315	**48**	TFTLTGF----------LIPTIID	**64**	*Synechococcus* sp. *JA-3-3Ab*
gi|123502915	**48**	TFTLTGF----------LIPTIID	**64**	*Synechococcus* sp. *JA-2-3B'a(2-13)*
gi|81709614	**43**	TFTLTGF----------LIPTIID	**59**	*Gloeobacter violaceus PCC 7421*
gi|120541	**43**	TFTLTGF----------LIPTIID	**59**	*Chlamydomonas reinhardtii*
gi|13878446	**43**	TFALTGF----------LIPTIMD	**59**	*Nephroselmis olivacea*
gi|3023485	**43**	TFTLTGF----------LIPTIID	**59**	*Chlorella vulgaris*
gi|68052157	**43**	TFTLTGF----------LIPTIID	**59**	*Auxenochlorella protothecoides*
gi|182894146	**43**	TFTLTGF----------LIPTIID	**59**	*Leptosira terrestris*
gi|122165109	**43**	TFTLTGF----------LIPTIID	**59**	*Stigeoclonium helveticum*
gi|122179518	**43**	TFTLTGF----------LIPTIID	**59**	*Scenedesmus obliquus*
gi|1345782	**43**	TFTLTGH----------LIPTIID	**59**	*Cyanophora paradoxa*
gi|122195140	**43**	TFTLTGF----------LIPTIID	**59**	*Oltmannsiellopsis viridis*
gi|544021	**48**	TFTLTGF----------LIPTIID	**64**	*Polystichum acrostichoides*
gi|254810211	**45**	TFPLTGH----------LQPTVID	**61**	*Chloroflexus sp. Y-400-fl*
gi|13878340	**45**	TFPLTGH----------LQPTVID	**61**	*Chloroflexus aurantiacus J-10-fl*
gi|254810210	**45**	TFPLTGH----------LQPTVID	**61**	*Chloroflexus aggregans DSM 9485*

Table 1 continues on the next page

Table 1 (continued)

GI number L subunit of DPOR	Amino acid sequence			Organism
gi|189081504	**45**	TFALTGM----------LQPTVID	**61**	*Roseiflexus castenholzii DSM 13941*
gi|166224350	**45**	TFALTGT----------LQPTVID	**61**	*Roseiflexus* sp. *RS-1*
gi|226698868	**45**	TFPLTGT----------LQKTVIE	**61**	*Prosthecochloris aestuarii DSM 271*
gi|226698864	**45**	TFPLTGT----------LQKTVIE	**61**	*Chlorobium phaeobacteroides BS1*
gi|226698862	**45**	TFPITGK----------LQKTVIE	**61**	*Chlorobium limicola DSM 245*
gi|166224347	**45**	TFPITGK----------LQKTVIE	**61**	*Chlorobium phaeobacteroides DSM 266*
gi|189081503	**45**	TFPITGK----------LQKTVIE	**61**	*Chlorobium phaeovibrioides DSM 265*
gi|226698867	**45**	TFPITGK----------LQKTVIE	**61**	*Pelodictyon phaeoclathratiforme BU-1*
gi|123579265	**45**	TFPITGK----------LQKTVIE	**61**	*Chlorobium chlorochromatii CaD3*
gi|123583565	**45**	TFPITGK----------LQKTVIE	**61**	*Chlorobium luteolum DSM 273*
gi|226698863	**45**	TFPITGK----------LQKTVIE	**61**	*Chlorobaculum parvum NCIB 8327*
gi|13878343	**45**	TFPITGK----------LQKTVIE	**61**	*Chlorobium tepidum TLS*
gi|226698865	**45**	TFPITGH----------LQKTVIE	**61**	*Chloroherpeton thalassium ATCC 35110*
gi|170652908	**76**	TFTLTGS----------LVPTVID	**92**	*Dinoroseobacter shibae DFL 12*
gi|157913837	**76**	TFTLTGS----------LVPTVID	**92**	*Dinoroseobacter shibae DFL 12*
gi|123066021	**76**	TFTLTGS----------LVPTVID	**92**	*Roseobacter denitrificans OCh 114*
gi|172046597	**83**	TFTLTGM----------LQPTVID	**99**	*Jannaschia* sp. *CCS1*
gi|114863	**79**	TFTLTGR----------LQETVID	**95**	*Rhodobacter capsulatus*
gi|254810219	**74**	TFTLTGS----------LVPTVID	**90**	*Rhodobacter sphaeroides KD131*
gi|166224348	**74**	TFTLTGS----------LVPTVID	**90**	*Rhodobacter sphaeroides ATCC 17029*
gi|85681290	**74**	TFTLTGS----------LVPTVID	**90**	*Rhodobacter sphaeroides 2.4.1*
gi|225734166	**91**	TFTLTGS----------LVPTVID	**107**	*Rhodobacter sphaeroides 2.4.1*
gi|225734165	**91**	TFTLTGS----------LVPTVID	**107**	*Rhodobacter sphaeroides 2.4.1*
gi|215261299	**84**	TFTLTGS----------LVPTVID	**100**	*Rhodobacter sphaeroides 2.4.1*
gi|215261298	**84**	TFTLTGS----------LVPTVID	**100**	*Rhodobacter sphaeroides 2.4.1*
gi|166224349	**74**	TFTLTGS----------LVPTVID	**90**	*Rhodobacter sphaeroides ATCC 17025*
gi|170652907	**78**	TFTLTKR----------LVPTVID	**94**	*Bradyrhizobium* sp. *ORS 278*
gi|170652906	**78**	TFTLTKR----------LVPTVID	**94**	*Bradyrhizobium* sp. *BTAi1*
gi|254810218	**80**	TFTLTKK----------LVPTVID	**96**	*Rhodospirillum centenum SW*
gi|123762521	**88**	TFTLTKR----------LIPTVID	**104**	*Rhodopseudomonas palustris BisB5*
gi|123292175	**88**	TFTLTKR----------LIPTVID	**104**	*Rhodopseudomonas palustris HaA2*
gi|122476964	**88**	TFTLTKR----------LVPTVID	**104**	*Rhodopseudomonas palustris BisB18*
gi|81698290	**88**	TFTLTKK----------LMPTVID	**104**	*Rhodopseudomonas palustris CGA009*
gi|122297133	**86**	TFTLTKC----------LIPTVID	**102**	*Rhodopseudomonas palustris BisA53*
gi|123527299	**72**	TFTLTKR----------LVPTVID	**88**	*Rhodospirillum rubrum ATCC 11170*
gi|13878351	**67**	TFTLTKR----------LVPTVID	**83**	*Rhodospirillum rubrum*
gi|13878348	**79**	TFTLTKR----------MVPTVID	**95**	*Rubrivivax gelatinosus*
gi|254810213	**74**	TFTLTKR----------LAPTVID	**90**	*Methylobacterium extorquens PA1*
gi|254810212	**74**	TFTLTKR----------LAPTVID	**90**	*Methylobacterium chloromethanicum CM4*
gi|254810214	**74**	TFTLTKR----------LAPTVID	**90**	*Methylobacterium populi BJ001*
gi|254810215	**74**	TFTLTKR----------LAPTVID	**90**	*Methylobacterium radiotolerans JCM 2831*
gi|254810216	**78**	TFTLTKR----------LAPTVID	**94**	*Methylobacterium* sp. *4-46*
gi|226706355	**72**	TFTLTHK----------MVPTVID	**88**	*Prochlorococcus marinus str. MIT 9211*
gi|81712822	**72**	TFTLTHK----------MVPTVID	**88**	*Prochlorococcus marinus subsp. marinus str. CCMP1375*
gi|182894152	**72**	TFTLTHK----------MVPTVID	**88**	*Prochlorococcus marinus* str. *NATL1A*
gi|123620280	**72**	TFTLTHK----------MVPTVID	**88**	*Prochlorococcus marinus* str. *NATL2A*
gi|182894151	**72**	TFTLTHR----------MVPTVID	**88**	*Prochlorococcus marinus* str. *MIT 9303*
gi|81712691	**72**	TFTLTHR----------MVPTVID	**88**	*Prochlorococcus marinus* str. *MIT 9313*
gi|182894150	**72**	TFTLTHK----------MVPTVID	**88**	*Prochlorococcus marinus* str. *MIT 9301*
gi|182894148	**72**	TFTLTHK----------MVPTVID	**88**	*Prochlorococcus marinus* str. *AS9601*
gi|172047292	**72**	TFTLTHK----------MVPTVID	**88**	*Prochlorococcus marinus* str. *MIT 9215*
gi|123554484	**72**	TFTLTHK----------MVPTVID	**88**	*Prochlorococcus marinus* str. *MIT 9312*
gi|182894149	**72**	TFTLTHK----------MVPTVID	**88**	*Prochlorococcus marinus* str. *MIT 9515*
gi|81712619	**72**	TFTLTHK----------MVPTVID	**88**	*Prochlorococcus marinus* subsp. *pastoris str. CCMP1986*

Table 1 continues on the next page

Table 1 (continued)

GI number		Amino acid sequence		Organism
L subunit of DPOR				
gi|123578595	**72**	TFTLTHK----------MVPTVID	**88**	*Synechococcus* sp. *CC9605*
gi|81574172	**72**	TFTLTHK----------MVPTVID	**88**	*Synechococcus* sp. *WH 8102*
gi|172047785	**72**	TFTLTHK----------MVPTVID	**88**	*Synechococcus* sp. *WH 7803*
gi|172046629	**72**	TFTLTHS----------MVPTVID	**88**	*Synechococcus* sp. *CC9902*
gi|123327701	**72**	TFTLTHK----------MVPTVID	**88**	*Synechococcus* sp. *CC9311*
gi|172047910	**76**	TFTLTHK----------MVPTVID	**92**	*Synechococcus* sp. *RCC307*
gi|254810217	**79**	TFTLTKR----------FVPTVID	**95**	*Methylocella silvestris BL2*
gi|170652909	**77**	TFTLTKR----------LVPTVID	**93**	*Halorhodospira halophila SL1*
LPOR				
gi|10720232	**182**	RFTADGFELSVGTNHLGHFLLTNLLLD	**208**	*Chlamydomonas reinhardti i*
gi|1408176	**182**	RFTADGFELSVGTNHLGHFLLTNLLLD	**208**	*Chlamydomonas reinhardtii*
gi|3327258	**242**	KFSAEGFELSVGTNHMGHFLLARLLME	**268**	*Marchantia paleacea* subsp. *diptera*
gi|10720231	**242**	KFSAEGFELSVGTNHMGHFLLARLLME	**268**	*Marchantia paleacea*
gi|15218860	**186**	SFTAEGFEISVGTNHLGHFLLSRLLLD	**212**	*Arabidopsis thaliana*
gi|10720234	**186**	SFTAEGFEISVGTNHLGHFLLSRLLLD	**212**	*Arabidopsis thaliana*
gi|8467964	**186**	SFTAEGFEISVGTNHLGHFLLSRLLLD	**212**	*Arabidopsis thaliana*
gi|79316418	**184**	SFTAEGFEISVGTNHLGHFLLSRLLLD	**210**	*Arabidopsis thaliana*
gi|297843168	**186**	SFTAEGFELSVGTNHLGHFLLSRLLLD	**212**	*Arabidopsis lyrata subsp. lyrata*
gi|297335307	**186**	SFTAEGFELSVGTNHLGHFLLSRLLLD	**212**	*Arabidopsis lyrata subsp. lyrata*
gi|75248671	**182**	SFTADGFEMSVGVNHLGHFLLARELLA	**208**	*Oryza sativa Japonica Group*
gi|115482724	**68**	SFTADGFEMSVGVNHLGHFLLARELLA	**94**	*Oryza sativa Japonica Group*
gi|113639564	**68**	SFTADGFEMSVGVNHLGHFLLARELLA	**94**	*Oryza sativa Japonica Group*
gi|10720236	**179**	SFTADGFEMSVGVNHLGHFLLARELLE	**205**	*Hordeum vulgare*
gi|46019982	**155**	SYTADGFEMSVGVNHLGHFLLARELLS	**181**	*Zea mays*
gi|79325287	**185**	TYSAEGFELSVATNHLGHFLLARLLLD	**211**	*Arabidopsis thaliana*
gi|15234129	**185**	TYSAEGFELSVATNHLGHFLLARLLLD	**211**	*Arabidopsis thaliana*
gi|1583456	**185**	TYSAEGFELSVATNHLGHFLLARLLLD	**211**	*Arabidopsis thaliana*
gi|2507092	**185**	TYSAEGFELSVATNHLGHFLLARLLLD	**211**	*Arabidopsis thaliana*
gi|968977	**185**	TYSAEGFELSVATNHLGHFLLARLLLD	**211**	*Arabidopsis thaliana*
gi|15239574	**189**	TFTAEGFELSVGINHLGHFLLSRLLID	**215**	*Arabidopsis thaliana*
gi|26454645	**189**	TFTAEGFELSVGINHLGHFLLSRLLID	**215**	*Arabidopsis thaliana*
gi|1583455	**189**	TFTAEGFELSVGINHLGHFLLSRLLID	**215**	*Arabidopsis thaliana*
gi|968975	**189**	TFTAEGFELSVGINHLGHFLLSRLLID	**215**	*Arabidopsis thaliana*
gi|79330812	**68**	TFTAEGFELSVGINHLGHFLLSRLLID	**94**	*Arabidopsis thaliana*
gi|10720220	**183**	TFTAEGFELSVGTNHLGHFLLSRLLLE	**209**	*Cucumis sativus*
gi|2244614	**183**	TFTAEGFELSVGTNHLGHFLLSRLLLE	**209**	*Cucumis sativus*
gi|9587209	**182**	THTADGFELSVGTNHLGHFLLSRLLLE	**208**	*Vigna radiata*
gi|10720233	**182**	TYTADGFELSVGTNHLGHFLLSRLLLD	**208**	*Daucus carota*
gi|266742	**183**	SFTADGFEISVGTNHLGHFLLSRLLLE	**209**	*Pisum sativum*
gi|20830	**183**	SFTADGFEISVGTNHLGHFLLSRLLLE	**209**	*Pisum sativum*
gi|227065	**171**	TFTADGHEMSVGVNHLGHFLLARLLME	**197**	*Hordeum vulgare* subsp. *vulgare*
gi|129708	**171**	TFTADGHEMSVGVNHLGHFLLARLLME	**197**	*Hordeum vulgare*
gi|10720235	**171**	TFTADGHEMSVGVNHLGHFLLARLLME	**197**	*Triticum aestivum*
gi|129707	**96**	TFTAEGVEMSVGVNHLGHFLLARLLLE	**122**	*Avena sativa*
gi|75232717	**170**	TFTADGYEMSVGVNHLGHFLLARLMLD	**196**	*Oryza sativa Japonica Group*
gi|115461348	**170**	TFTADGYEMSVGVNHLGHFLLARLMLD	**196**	*Oryza sativa Japonica Group*
gi|113565845	**170**	TFTADGYEMSVGVNHLGHFLLARLMLD	**196**	*Oryza sativa Japonica Group*
gi|2598163	**49**	TFTAEGFELSVGTNHLGHFLLSRLLLE	**75**	*Oryza sativa Japonica Group*
gi|7330644	**184**	TYTAEGFELSVGTNHLGHFLLSRLLLE	**210**	*Pinus mugo*
gi|226515427	**157**	TYTKDGFEETVGVTHLGHFLLANLMLK	**183**	*Micromonas* sp. *RCC299*
gi|255072981	**157**	TYTKDGFEETVGVTHLGHFLLANLMLK	**183**	*Micromonas* sp. *RCC299*

Statistical analysis included calculation of the number of sequences having a given residue at each position in the sequence with respect to the total number of the sequences in the constructed protein database for LPOR and BchL/ChlL sequences separately. This provided information about the frequency of the occurrence of a given amino acid residue at a certain position in the identified motif.

Modeling of the tertiary structure of LPOR: The tertiary structure of *A. thaliana* PORA (NCBI accession number: NP_200230) was predicted by homology modeling. The modeling templates were identified within PDB deposed proteins and 3 templates with the highest sequence homology to *A. thaliana* PORA were used, *i.e.*, porcine testicular carbonyl reductase (pdb:1n5d), gluconate 5-dehydrogenase TM0441 *Thermotoga maritima* (pdb: 1vl8) and human carbonyl reductase 3, complexed with $NADP^+$ (pdb:2hrb). The modeling was performed by SwissMODEL (Arnold *et al.* 2006) and *Modeller 9v8* (John and Šali 2003) for comparison.

Results and discussion

Newly identified amino acid motif in LPOR and the L subunit of DPOR: The comparison of amino acid sequences of *A. thaliana* PORA (NCBI accession number: NP_200230) with BchL/ChlL from the NCBI protein data bank showed a fragment consisting of 14 amino acid residues similar in PORA of *A. thaliana* and all the investigated BchL/ChlL sequences. In the case of *A. thaliana* PORA, the motif (called TFT) showed the following sequence: TFTAEGF-X-LSRLLLD, where -X- was the insert of 13 amino acids not found in the investigated BchL/ChlL sequences (Fig. 2). The identified fragment was then found in all of the investigated plants' LPOR sequences from the NCBI protein data bank. It should be explained that in the search, not only did we focus on finding identical amino acids at a given position in the TFT motif, but we also accepted residues having similar physicochemical character of amino acid side groups.

The summary of amino acid sequence of the TFT motif obtained for the BchL/ChlL and for LPOR sequences is presented in Fig. 3. Threonine and threonine/serine, *i.e.* the amino acids containing hydroxyl group, were found in the 1st position of the TFT motif in all BchL/ChlL and in the majority of LPOR sequences. Arginine or lysine were identified only in four LPOR sequences. Phenylalanine was in 2nd position in all of BchL/ChlL sequences and in 74% of LPOR sequences. In 24% of LPOR sequences, phenylalanine was replaced by tyrosine. Threonine/serine always occurred in the 3rd position in LPOR sequences and in most of BchL/ChlL sequences (85%). In the latter case, apart from threonine, either proline (12 %) or alanine (3%) were identified. In the 4th position, mostly hydrophobic amino acids were found, *i.e.* leucine/isoleucine in BchL/ChlL, and alanine in LPOR sequences. Aspartic or glutamic acids were found in 5th position in all of the LPOR sequences, whereas threonine was detected at this position in 98% of the investigated BchL/ChlL sequences. The next two positions in the TFT motif were more conserved in LPOR, having only glycine in 6th and mostly phenylalanine in 7th position, than in BchL/ChlL in which these two amino acids were also found at respective positions, however, with much lower frequency. The second part of the TFT motif, preceded by the insert in the case of LPOR, started with leucine in 8th position in all the LPOR sequences and in 78 % of BchL/ChlL sequences. The residues in the next three positions (9–11) differed between BchL/ChlL and LPOR (Fig. 3). The positions no. 12 and 13 were occupied by hydrophobic amino acids, namely, valine or isoleucine in BchL/ChlL and most frequently by leucine in LPOR or less frequently by methionine. Acidic amino acids (aspartic or glutamic) at the last position were found in all the BchL/ChlL sequences, as well as in most of (85%) the LPOR sequences.

Although the TFT motif is not homological between BchL/ChlL and LPOR sequences, the similar physicochemical character of amino acids in respective positions of the motif (in case of LPOR and BchL/ChlL sequences) was observed for 9 out of 14 residues. This provides similar properties of microenvironment created by amino acids of this motif for both oxidoreductases. Assuming a random selection of 14-amino acid length fragment, as well as equal likelihood for each residue in each position of the motif, the probability of the occurrence of an identical motif is 0.2×10^{-7}. The TFT motif contains polar amino acids with hydroxyl groups that can form hydrogen bonds and aromatic residues that are able to interact with the porphyrin ring of Pchlide molecule (Fig. 3). An insert in the TFT motif found in all the investigated LPOR sequences (Fig. 3*B*) included hydrophilic (S, T), hydrophobic (L, I, V) and aromatic (F, Y) amino acids, as well as histidine. As it can be calculated on the basis of the data shown in Fig. 3*B*, 54% (*i.e.* 7 from 13) of the residues within LPOR insert were conserved.

The presence of the TFT motif was also checked in SDR proteins and Fe protein of nitrogenase (NifH) using LPOR and BchL/ChlL as a reference, respectively. However, no fragments similar to the TFT motif were observed either in SDR or in NifH sequences (Fig. 2). Therefore, this motif may be involved in the functioning of LPOR and DPOR proteins. Obviously, to find out the physiological role of this motif in two Pchlide reductases, additional experimental data are required. However, among the already published results, some experimental evidence can be found for the significance of the TFT region for LPOR enzymatic activity. For example, Dahlin *et al.* (1999) showed that clustered charge-to-alanine mutagenesis, *i.e.* change of two charged residues to alanines in the DGFE and HLGH motifs of the LPOR sequence resulted in a complete loss of the enzyme activity. The modified fragments corresponded to the positions 5-6-7-1_i and 8_i-9_i-10_i-11_i (Fig. 3) of the TFT motif, respectively. Moreover, inhibition of the LPOR activity was found in the case of mutations of the R or D residues that are localized at the 10th and 14th positions of the TFT motif, respectively.

Fig. 2. Protein sequence alignment of NifH from *Clostridium pasteurianum*, BchL form *Rhodobacter capsulatus*, PORA from *Arabidopsis thaliana* and SDR4 (carbonyl reductase) from *Sus scrofa*. In the case of POR and SDR, characteristic motifs: NAA (NADPH-binding) and YxxxK (catalytic) are indicated.

The TFT motif in the homology model of *A. thaliana* PORA: In LPOR sequences (Fig. 2), the TFT motif was found between the NAA motif, which is one of NADPH-binding sites, and the catalytic YxxxK motif (Yang and Cheng 2004). Unfortunately, there are no crystal or NMR structures of LPOR published so far, thus all assumptions need to be made based on homology modeling of known SDR structures. In the present work, we have modeled a representation of the tertiary structure of PORA from *A. thaliana* (NCBI accession number NP_200230) that has not been modeled until now. There were no significant differences between the models obtained by SwissMODEL and Modeller software in the SDR-homologous regions.

All typical features of SDR (Oppermann *et al.* 2003) were found in the obtained model (Fig. 4*A*), *i.e.* two long helices are facing a 7-stranded β-sheet and 7 shorter helices. The origin of the TFT motif (*i.e.* T-F-T sequence) was localized on the top of one of the long helices, called αD in the SDR helix numbering (Oppermann *et al.* 2003),

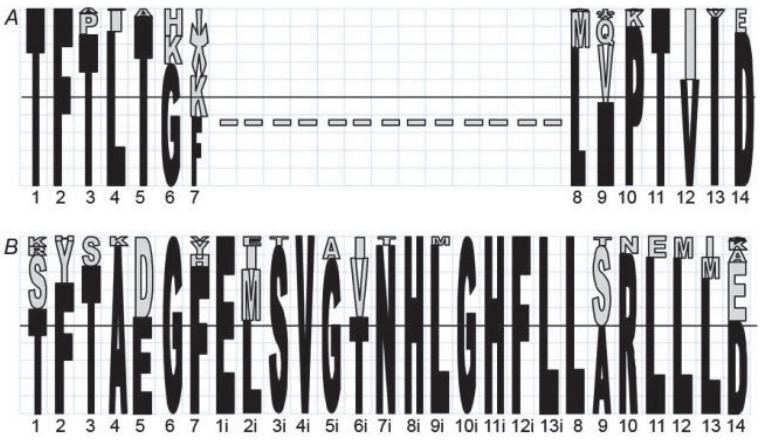

Fig. 3. TFT amino acid motif in BchL/ChlL (*A*) and plant LPOR (*B*). Residues in the insert of LPOR were numbered separately; 'i' stands for insert. Heights of the letters correspond to the frequency of the occurrence of a given amino acid at the given position within the TFT motif calculated for all sequences from each sequence group. The 50% frequency level is marked as the black horizontal line. Asterisk stands for amino acids occurring at a very low frequency.

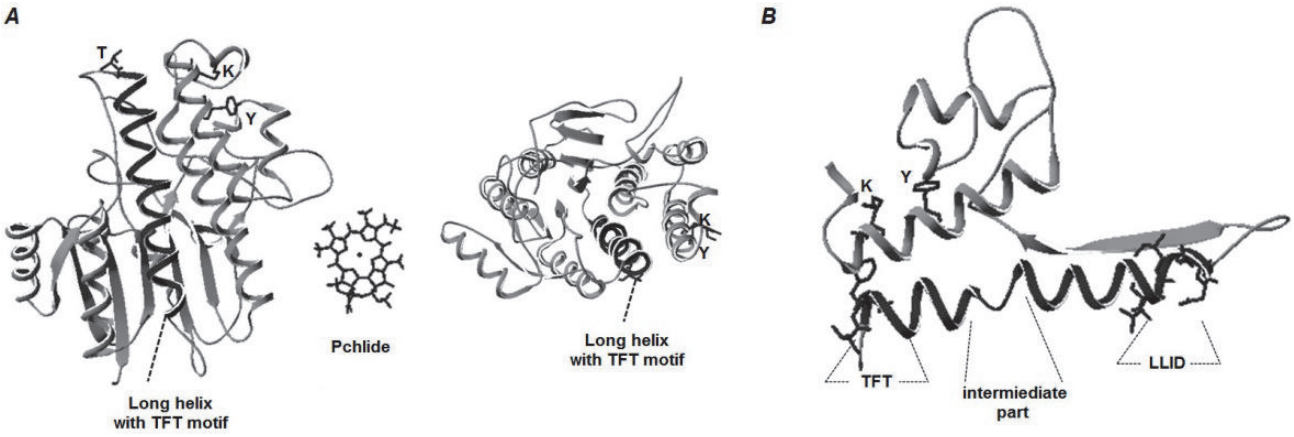

Fig. 4. *A*: The model of PORA from *Arabidopsis thaliana*: side view (*left*), top view (*right*) and Pchlide molecule (*middle*). The TFT motif was shown as a single helix. Tyrosine and lysine residues are at positions 280 and 284, respectively, corresponding to Y275 and K279 in the catalytic motif (YxxxK) of barley PORB (Lebedev *et al*. 2001) are marked. The estimated distance between the first and the last residues of the motif is 29 Å. For details *see* the text. *B*: The fragment of *A. thaliana* LPOR structure, containing the TFT motif with marked T-F-T and L-L-I-D sequences. The internal part of the long helix represents a fragment with a coil structure.

and the whole TFT motif was in this helix. However, the helical structure of this region seems to be forced by the spatial orientation of adjacent elements of the protein structure. When only the fragment of the PORA sequence (90–220 amino acid) was modeled, the central region of the long helix (199–208 amino acid), marked as 'intermediate region' in Fig. 4*B*, was evidently shown to be an unstructured loop splitting the long helix into two short helices. Using algorithms for protein secondary structure prediction (*e.g*. GOR4 - Garnier *et al.* 1996, and JUFO - Meiler and Baker 2003), it was also found, with high probability, that these regions are unstructured (not shown).

In the known homology models of LPOR from *Synechocystis* (Townley *et al.* 2001) and barley (Buhr *et al.* 2008), the TFT motif was found within the longest α-helix, like in our model. On the other hand, different conformation of this motif was identified in the 'old' model of pea LPOR (Dahlin *et al.* 1999) where only a part of the TFT motif adopted the helical structure. However, the modeling of the pea LPOR sequence, using the same algorithm that we used for *A. thaliana* LPOR, gave similar conformation of the TFT motif like that of *A. thaliana* (results not shown). The different structure obtained by Dahlin *et al.* (1999) might have resulted from template selection or from older algorithms introduced into *Modeller 3* and *Modeller 8* softwares than those used in the present work.

In the *Arabidopsis* PORA model, the TFT motif is located in close proximity of the highly conserved Y280 and K284 residues (Fig. 4). This YxxxK motif was shown to be indispensable for catalytic activity of LPOR, where Y residue has been suggested as direct proton donor to C18 during the reduction of Pchlide, and K is supposed to be important in facilitating deprotonation of Y (Wilks and Timko 1995, Lebedev *et al.* 2001, Heyes and Hunter 2002). In the presently modeled conformation, the threonine in 3rd position of the TFT motif faces one of the cysteine residues (Cys-222 in *Synechocystis* POR, which is equivalent to Cys-313 in *A. thaliana* POR), located on the next helix (at the distance of 4Å). This cysteine is suggested to be protected from oxidation when NADPH is bound (Heyes *et al.* 2000).

It has recently been demonstrated that binding of Pchlide to LPOR protein occurs *via* strong hydrogen bonds (Sytina *et al.* 2010 and 2011), which was earlier suggested by Solymosi *et al.* (2002). Several fragments of the Pchlide molecule, involving carbonyl groups and Mg (Fig. 1) may form hydrogen bonds directly or indirectly with methanol molecules (Zhao and Han 2008). Absorption and fluorescence properties of Pchlide (Mysliwa-Kurdziel *et al.* 2004, 2008), as well as its excited-state relaxation (Dietzek *et al.* 2006, 2009, 2010), were shown to be influenced by its interaction with hydroxyl group-binding solvents. Pchlide of etioplast inner membranes, where it naturally accumulates during etiolation (Solymosi and Schoefs 2010), showed similar spectroscopic properties to those found in protic solvents (Mysliwa-Kurdziel *et al.* 1999). Another observation worth mentioning is the presence of two highly conservative histidinyl residues in the LPOR insert (Fig. 3*B*), which may provide a coordination site for the Mg of the Pchlide molecule. Sytina *et al.* (2011) have recently demonstrated hexacoordination of the LPOR-bound Pchlide.

All of these data indicate the importance of the polarity of the local microenvironment for the excited-state properties of Pchlide, that are in turn crucial for its photoreduction catalyzed by LPOR. It has not yet been revealed which sites of LPOR molecule participate in the formation of hydrogen-bond network that stabilizes Pchlide molecule and to what extent hydroxyl group-binding residues of the TFT motif might contribute to this process.

Binding of NADPH to LPOR precedes and probably facilitates Pchlide binding during assembly of the substrate-enzyme complex and induces conformational changes of LPOR (Heyes and Scrutton 2009; Sytina *et al.* 2008, 2009). These changes influence distances and relative temporary orientation of the single residues of LPOR protein. Interaction of amino acid residues of the TFT motif with Pchlide molecule is possible, especially when taking into account the helix-loop-helix conformation of the motif (Fig. 4*B*).

In angiosperms, Pchlide:LPOR:NADPH complex forms aggregates *in vivo* and it is widely accepted that activity of these ternary complexes is conferred by their aggregation (Schoefs and Franck 2003, Schoefs 2005). Dimerization/oligomerization of LPOR:Pchlide:NADPH complexes was also demonstrated in some *in vitro* experiments performed on LPOR of angiosperms (Wiktorsson *et al.* 1992, Martin *et al.* 1997, Ouazzani-Chahdi *et al.* 1998). It is still unknown how LPOR monomers are oriented in the dimer/oligomer and which parts of the LPOR molecule participate in the dimerization/oligomerization process. However, it is worth mentioning that long helices are considered to be the main interaction interface in oligomeric SDRs (Filling *et al.* 2002). If so, a possibility to consider is the interaction of two POR monomers with their long helices in head-to-tail orientation.

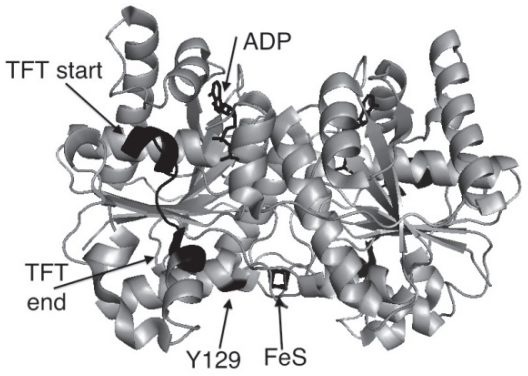

Fig. 5. Crystal structure of L-DPOR from *Rhodobacter sphaeroides* (pdb: 3FWY, Sarma et al. 2008) with FeS cluster and ADP marked. Tyrosine Y129 is supposed to be important for the interaction between the $[BchL]_2$ and $[BchN\text{-}BchB]_2$. TFT and TVID correspond to the origin and to the end of TFT motif, respectively. The figure was generated with *PyMol* (*The PyMOL Molecular Graphics System, v. 0.99rc6, Schrödinger, LLC*, San Carlos, CA, USA).

The TFT motif in BchL: Concerning the crystal structure of BchL from *Rhodobacter sphaeroides* (Sarma *et al.* 2008), the TFT motif can be found in the outer layer of the protein molecule (Fig. 5), close to the tyrosine (*i.e.* Y129), being important for the interaction between the $[BchL]_2$ and $[BchN\text{-}BchB]_2$ subunits of DPOR. The middle part of the TFT motif is found mostly in the unstructured fragment of the protein, whereas the beginning and the end adopt the helix structure. The recently published crystal structure of the $[BchN\text{-}BchB]_2$ heterotetramer from *Rhodobacter capsulatus* (Muraki *et al.* 2010) revealed that Pchlide is bound on the interface of heterotetramer consisting of two catalytic [BchN-BchB] heterodimers, in a cavity formed by hydrophobic amino acids, without any involvement of the BchL in the process. Nevertheless, the C-terminal fragment of BchB, which is well conserved and probably important for Pchlide reduction, remains unresolved in the obtained structure and was described as disordered (Muraki *et al.* 2010).

On the other hand, biochemical studies showed that the interaction between the L-protein and the catalytic NB-protein was essential for Pchlide reduction (Nomata *et al.* 2008, Bröcker *et al.* 2008, Wätzlich *et al.* 2009). Binding of Pchlide to the NB-protein was required for the whole DPOR complex formation (Bröcker *et al.* 2010*b*). It was recently shown that this binding was the initial step of DPOR catalysis, which promotes docking of the L-protein to the NB-protein, and is followed by ATP hydrolysis and Pchlide reduction (Bröcker *et al.* 2008, 2010b).

Even though the catalytic mechanism of DPOR has been proposed and the crystal structure of DPOR subunits has been resolved, the structure and the molecular mechanism of the assembly of the whole DPOR complex have not been elucidated until now. In particular, the mechanism of docking of $[BchL]_2$ dimer to $[BchN\text{-}BchB]_2$

Fig. 6. Glycine-rich motif of LPOR (*A*), SDR (*B*), L subunit of DPOR (*C*) and NifH (*D*). Heights of the letters correspond to the frequency of the occurrence of a given amino acid at the given position within the glycine-rich motif calculated for all sequences from each sequence group. The 50% frequency level is marked as the black horizontal line. Asterisks stand for amino acids occurring at very low frequency. The analysis was performed on protein sequences found in NCBI.

heterotetramer and that of Pchlide (and Chlide)-enzyme interactions in DPOR complex still need detailed investigation. With the currently available data, one can only speculate that the TFT motif may play a role in docking of the L-protein to the NB-protein, for example by interacting with Pchlide molecule already bound to the BchN-BchB dimer. Pchlide might occur in the cavity formed by the BchN-BchB dimer and BchL- interface if we allow the possibility of different docking of the L-protein as opposed to the one proposed on the basis of the comparison with the nitrogenase enzyme complex. Sarma *et al.* (2008) have noticed some structural differences between the docking surface of the NifH and the respective fragments of BchL. It has to be taken into consideration that, although the homology between nitrogenase and DPOR is high, their substrates are completely different. Bröcker *et al.* (2010a) have also suggested that the common ancestor of DPOR and nitrogenase is an unknown nitrogenase-like protein.

Glycine-rich motif: Both LPOR and the BchL/ChlL subunits of DPOR are able to bind NADPH and ATP, respectively, that is important for their catalytic activity. In the case of LPOR, the presence of the conserved NADPH binding motif, *i.e.* GxxxGxG, was one of the reasons for their classification as an SDR protein (Wilks and Timko 1995). Our investigation showed 100% homology for all the residues of the motif in the investigated LPOR sequences (Fig. 6*A*), meaning that it was more conserved than those described for SDR proteins (Fig. 6*B*). The highly conserved glycine-rich motif YGKGGIGKST (Fig. 6*C*,*D*) that is involved in ATP binding by the BchL of DPOR and NifH of nitrogenase, resembles GxGxxG motif characteristic for the dinucleotide-binding motif found in the family of medium-chain dehydrogenases/reductases (Benach *et al.* 2001). The occurrence of glycine rich motifs both in the L subunit of DPOR and in LPOR is an example of a wider convergence resulting from specific physicochemical and steric demands of the nucleotide-binding site.

Conclusions: In the present paper, we have identified the fragment of amino acid sequence, called TFT motif, having similar physicochemical properties in LPOR and in the L subunit of DPOR proteins. We have indicated a possible significance of this motif with regard to some known facts about LPOR and DPOR proteins. The current findings are important for the following future investigations: (*1*) mutagenesis experiments on the function of specific amino acids and (*2*) biochemical and biophysical studies aimed at revealing the molecular mechanism of the assembly of DPOR complex, as well as LPOR aggregation in prolamellar bodies. Moreover, it was interesting to show similarity of the two oxidoreductases generally regarded as completely unrelated. This observation may be important in detailed elucidation of the evolutionary origin of the two different protochlorophyllide oxidoreductases.

References

Arnold, K., Bordoli, L., Kopp, J., Schwede, T.: The SWISS-MODEL workspace: A web-based environment for protein structure homology modeling. – Bioinformatics **22**: 195-201, 2006.

Belyaeva, O.B., Litvin, F.F.: Photoactive pigment–enzyme complexes of chlorophyll precursor in plant leaves. – Biochemistry Moscow **72**: 1458-1477, 2007.

Benach, J., Atrian, S., Ladenstein, R., Gonzàlez-Duarte, R.: Genesis of *Drosophila* ADH: the shaping of the enzymatic activity from a SDR ancestor. – Chem-Biol Interactions **130-132**: 405-415, 2001.

Bröcker, M.J., Schomburg, S., Heinz, D.W., Jahn, D., Schubert, W.D., Moser, J.: Crystal structure of the nitrogenase-like dark operative protochlorophyllide oxidoreductase catalytic complex $(ChlN/ChlB)_2$. – J. Biol. Chem. **285**: 27336-27345, 2010a.

Bröcker, M.J., Virus, S., Ganskow, S., Heathcote, P., Heinz, D.W., Schubert, W.D., Jahn, D., Moser, J.: ATP-driven reduction by dark-operative protochlorophyllide oxidoreductase from *Chlorobium tepidum* mechanistically resembles nitrogenase catalysis. – J. Biol. Chem. **283**: 10559-10567, 2008.

Bröcker, M.J., Wätzlich, D., Saggu, M., Lendzian, F., Moser, J., Jahn, D.: Biosynthesis of (Bacterio)chlorophylls. ATP-dependent transient subunit interaction and electron transfer of dark operative protochlorophyllide oxidoreductase. – J. Biol. Chem. **285**: 8268-8277, 2010b.

Buhr, F., El Bakkouri, M., Valdez, O., Pollmann, S., Lebedev, N., Reinbothe, S., Reinbothe, C.: Photoprotective role of NADPH:protochlorophyllide oxidoreductase A. – Proc. Nat. Acad. Sci. USA **105**: 12629-12634, 2008.

Dahlin, C., Aronsson, H., Wilks, H., Lebedev, N., Sundqvist, C., Timko, M.P.: The role of protein surface charge in catalytic activity and chloroplast membrane association of the pea NADPH: protochlorophyllide oxidoreductase (POR) as revealed by alanine scanning mutagenesis. – Plant Mol. Biol. **39**: 309-323, 1999.

Dietzek, B., Kiefer, W., Popp, J., Hermann, G., Schmitt, M.: Solvent effects on the excited-state processes of protochlorophyllide: A femtosecond time-resolved absorption study. – J. Phys. Chem. **110**: 4399-4406, 2006.

Dietzek, B., Tschierlei, S., Hermann, G., Yartsev, A., Pascher, T., Sundstrom, V., Schmitt, M., Popp, J.: Protochlorophyllide *a*: a comprehensive photophysical picture. – Chem. Phys. Phys. Chem. **10**: 144-150, 2009.

Dietzek, B., Tschierlei, S., Hanf, R., Seidel, S., Yartsev, A., Schmitt, M., Hermann, G., Popp, J.: Dynamics of charge separation in the excited-state chemistry of protochlorophyllide. – Chem. Phys. Lett. **492**: 157-163, 2010.

Filling, C., Berndt, K.D., Benach, J., Knapp, S., Prozorowski, T., Nordling, E., Ladenstein, R., Jornvall, H., Oppermann, U.: Critical residues for structure and catalysis in short-chain dehydrogenases/reductases. – J. Biol. Chem. **277**: 25677-25684, 2002.

Garnier, J., Gibrat, J.F., Robson, B.: GOR method for predicting protein secondary structure from amino acid sequence. – In: Doolittle, R.F. (ed.): Methods in Enzymology **266**: 540-553, 1996.

Heyes, D.J., Hunter, C.N.: Site-directed mutagenesis of Tyr-189 and Lys-193 in NADPH: protochlorophyllide oxidoreductase from *Synechocystis*. – Biochem. Soc. Trans. **30**: 601-604, 2002.

Heyes, D.J., Hunter, C.N.: Making light work of enzyme catalysis: protochlorophyllide oxidoreductase. – Trends Plant Sci. **30**: 642-649, 2005.

Heyes, D.J., Martin, G.E., Reid, R.J., Hunter, C.N., Wilks, H.M.: NADPH:protochlorophyllide oxidoreductase from *Synechocystis*: overexpression, purification and preliminary characterisation. – FEBS Lett. **483**: 47-51, 2000.

Heyes, D.J., Scrutton, N.S.: Conformational changes in the catalytic cycle of protochlorophyllide oxidoreductase: what lessons can be learnt from dihydrofolate reductase? – Biochem. Soc. Trans. **37**: 354-357, 2009.

Igarashi, R.Y., Seefeldt, L.C.: Nitrogen fixation: the mechanism of the Mo-dependent nitrogenase. – Crit. Rev. Biochem. Mol. Biol. **38**: 351-381, 2003.

John, B., Šali, A.: Comparative protein structure modeling by iterative alignment, model building and model assessment. – Nucl. Acids Res. **31**: 3982-3992, 2003.

Lebedev, N., Karginova, O., McIvor, W., Timko, M.P.: Tyr275 and Lys279 stabilize NADPH within the catalytic site of NADPH:protochlorophyllide oxidoreductase and are involved in the formation of the enzyme photoactive state. – Biochemistry **40**: 12562-12574, 2001.

Martin, G.E., Timko, M.P., Wilks, H.M.: Purification and kinetic analysis of pea (*Pisum sativum* L.) NADPH:protochlorophyllide oxidoreductase expressed as a fusion with maltose-binding protein in *Escherichia coli*. – Biochem. J. **325**: 139-145, 1997.

Masuda, T.: Recent overview of the Mg branch of the tetrapyrrole biosynthesis leading to chlorophylls. – Photosynth. Res. **96**: 121-143, 2008.

Meiler, J., Baker, D.: Coupled prediction of protein secondary and tertiary structure. – Proc. Nat. Acad. Sci. USA **100**: 12105-12110, 2003.

Muraki, N., Nomata, J., Ebata, K., Mizoguchi, T., Shiba, T., Tamiaki, H., Kurisu, G., Fujita, Y.: X-ray crystal structure of the light-independent protochlorophyllide reductase. – Nature **465**: 110-114, 2010.

Mysliwa-Kurdziel, B., Franck, F., Strzałka, K.: Analysis of fluorescence lifetime of protochlorophyllide and chlorophyllide in isolated etioplast membranes measured from multifrequency cross-correlation phase fluorometry. – Photochem. Photobiol. **70**: 616-623, 1999.

Mysliwa-Kurdziel, B., Kruk, J., Strzałka, K.: Fluorescence lifetimes and spectral properties of protochlorophyllide in organic solvents and their relations to the respective parameters in vivo. – Photochem. Photobiol. **79**: 62-67, 2004.

Mysliwa-Kurdziel, B., Solymosi, K., Kruk, J., Böddi, B., Strzałka, K.: Solvent effects on fluorescence properties of protochlorophyll and its derivatives with various porphyrin side chains. – Eur. Biophys. J. **37**: 1185-1193, 2008.

Nomata, J., Ogawa, T., Kitashima, M., Inoue, K., Fujita, Y.: NB-protein (BchN–BchB) of dark-operative protochlorophyllide reductase is the catalytic component containing oxygen-tolerant Fe–S clusters. – FEBS Lett. **582**: 1346-1350, 2008.

Oppermann, U., Filling, C., Hult, M. *et al.*: Short-chain dehydrogenases/reductases (SDR): the 2002 update. – Chem-Biol. Interactions **143/144**: 247-253, 2003.

Ouazzani-Chahdi, M.A., Schoefs, B., Franck, F.: Isolation and characterization of photoactive complexes of NADPH:protochlorophyllide oxidoreductase from wheat. – Planta **206**: 673-680, 1998.

Pruitt, K.D., Tatusova, T., Maglott, D.R.: NCBI reference sequences (RefSeq): a curated non-redundant sequence database of genomes, transcripts and proteins. – Nucl. Acids Res. **35**: D61–D65, 2006.

Reinbothe, C., El Bakkouri, M., Buhr, F., Muraki, N., Nomata, J., Kurisu, G., Fujita, Y., Reinbothe, S.: Chlorophyll biosynthesis: spotlight on protochlorophyllide reduction. – Trends Plant Sci. **15**: 614-624, 2010.

Sarma, R., Barney, B.M., Hamilton, T.L., Jones, A., Seefeldt, L.C., Peters, J.W.: Crystal structure of the L protein of *Rhodobacter sphaeroides* light-independent protochlorophyllide reductase with MgADP bound: a homologue of the nitrogenase Fe protein. – Biochemistry **47**: 13004-13015, 2008.

Schoefs, B.: Protochlorophyllide reduction – what is new in 2005? – Photosynthetica **43**: 329-343, 2005.

Schoefs, B., Franck, F.: Protochlorophyllide reduction: mechanisms and evolution. – Photochem. Photobiol. **78**: 543-557, 2003.

Solymosi, K., Schoefs, B.: Etioplast and etio-chloroplast formation under natural conditions:the dark side of chlorophyll biosynthesis in angiosperms. – Photosynth. Res. **105**: 143-166, 2010.

Solymosi, K., Smeller, L., Böddi, B., Fidy, J.: Activation volumes of processes linked to the phototransformation of protochlorophyllide determined by fluorescence spectroscopy at high pressure. – Biochim. Biophys. Acta **1554**: 1-4, 2002.

Sytina, O.A., Alexandre, M.T., Heyes, D.J., Hunter, C.N., Robert, B., van Grondelle, R., Groot, M.L.: Enzyme activation and catalysis: characterisation of the vibrational modes of substrate and product in protochlorophyllide oxidoreductase. – Phys. Chem. Chem. Phys. **13**: 2307-2313, 2011.

Sytina, O.A., Heyes, D.J., Hunter, C.N., Alexandre, M.T., van Stokkum, I.H.M., van Grondelle, R., Groot, M.L.: Conformational changes in an ultrafast light-driven enzyme determine catalytic activity. – Nature **456**: 1001-1004, 2008.

Sytina, O.A., Heyes, D.J., Hunter, C.N., Groot, M.L:. Ultrafast catalytic processes and conformational changes in the light-driven enzyme protochlorophyllide oxidoreductase (POR). – Biochem. Soc. Trans. **37**: 387-391, 2009.

Sytina, O.A., van Stokkum, I.H.M., Heyes, D.J., Hunter, C.N., van Grondelle, R., Groot, M.L.: Protochlorophyllide excited-state dynamics in organic solvents studied by time-resolved visible and mid-infrared spectroscopy. – J. Phys. Chem. **114**: 4335-4344, 2010.

Thompson, J.D., Higgins, D.G., Gibson, T.J.: CLUSTAL W: improving the sensitivity of progressive multiple sequence alignment through sequence weighting, position-specific gap penalties and weight matrix choice. – Nucl. Acids Res. **22**: 4673-4680, 1994.

Townley, H.E., Sessions, R.B., Clarke, A.R., Dafforn, T.R., Griffiths, W.T.: Protochlorophyllide oxidoreductase: a homology model examined by site directed mutagenesis. – Proteins **44**: 329-335, 2001.

Wätzlich, D., Bröcker, M.J., Uliczka, F., Ribbe, M., Virus, S., Jahn, D., Moser, J.: Chimeric nitrogenase-like enzymes of (bacterio)chlorophyll biosynthesis. – J. Biol. Chem. **284**: 15530-15540, 2009.

Wiktorsson, B., Ryberg, M., Gough, S., Sundqvist, C.: Isoelectric focusing of pigment-protein complexes solubilized from non-irradiated and irradiated prolamellar bodies. – Physiol. Plant. **82**: 659-669, 1992.

Wilks, H.M., Timko, M.P.: A light-dependent complementation system for analysis of NADPH:protochlorophyllide oxidoreductase: Identification and mutagenesis of two conserved residues that are essential for enzyme activity. – Proc. Nat. Acad. Sci. USA **92**: 724-728, 1995.

Yang, J., Cheng, Q.: Origin and evolution of the light-dependent protochlorophyllide oxidoreductase (LPOR) genes. – Plant Biol. **6**: 537-544, 2004.

Zhao, G.J., Han, K.L.: Site-specific solvation of the photoexcited protochlorophyllide a in methanol: formation of the hydrogen-bonded intermediate state induced by hydrogen bond strengthening. – Biophys. J. **94**: 38-46, 2008.